International Journal of ISSI, Vol.3 (2006), No. 1, pp. 20-25

Stress- Corrosion Crack Initiation of High-strength Pipeline Steel in Near-neutral pH Environments

B. Fang[1], E-H. Han[2], M. Elboujdaini[3*], W. Zheng, J. Li[3] and R. W. Revie[3]

1- Environmental Corrosion Center, Institute of Metal Research,Chinese Academy of Science, Shenyang, P. R. China, 10016 and CANMET Materials Technology Laboratory, 568 Booth Street, Ottawa, Ontario, Canada K1A 0G1

2- Environmental Corrosion Center, Institute of Metal Research,Chinese Academy of Sciences, Shenyang, P. R. China, 10016

3- CANMET Materials Technology Laboratory, 568 Booth Street, Ottawa, Ontario, Canada K1A 0G1

Received June 20, 2006; Accepted July 25, 2006

Abstract

Stress-corrosion cracking (SCC) tests were conducted in the near-neutral pH standard solution, NS4, and in an actual soil solution, using four-point bending at a high stress ratio and low frequency conditions very similar to those of operational pipelines. Pitting incubation appeared first and then pitting initiated and grew in both solutions although there were many more pits on the specimen tested in soil purged with 5% CO_2 +95%N_2 than in the specimen tested in NS4 solution purged with the same gas. These observations show that samples in soil solution are more susceptible to pitting than those in NS4 solution. When the pit reached a critical size, the increased stress concentration around the pits, resulted in transition to a crack.

Keywords: Stress-corrosion cracking, High-strength, Pipeline.

Introduction

Stress-corrosion cracking (SCC) from the external side of pipeline (which is related to the holiday, deterioration and disbonded of coating, the applied cathodic protection current passing through the disbonded location, the coating shielding ability and the solution conductivity) is a serious problem for the pipline industry. Since the first failure case was documented in the 1960s[1)], many failures have occurred in gas and oil pipelines[2,3)].Several studies[4-6)] have been carried out to investigate the different factors including environmental conditions, pressure fluctuations, stress ratio, load-cycle frequency, strain rate and metallurgical parameters on SCC behavior. It is generally accepted that both hydrogen and dissolution are involved in the mechanism of near-neutral pH SCC, while grain boundaries could suffer from local attacks common in high-pH-SCC[7-8)]. Research reveals that SCC is engendered by a number of factors, of which two main contributors are stress in the pipe steel, and a particular type of corrosive environment around the pipe after the grade of pipeline steel is determined. Under certain conditions, what begins as a tiny hairline crack on the exterior of the pipe could become a 'colony' of cracks with the potential to penetrate the steel and cause the pipeline to rupture.

* *Corresponding author:*
Tel: (613) 992-9573 Fax : (613) 992-8735
E-mail: melboujd@nrcan.gc.ca
Address: CANMET Materials Technology Laboratory 568 Booth Street, Ottawa, Ontario, CANADA, K1A 0G1

Only limited literature is available about crack initiation and early-stage propagation of near-neutral-pH SCC[9-12)]. The crack-initiation sites are studied in detail, and are associated with non-metallic inclusions, pits, surface discontinuous defects and persistent slip bands produced by mechanical pre-treatment of the steel. There is also viable crack-probability model capable of predicting the initiation of near-neutral-pH SCC, and it includes separate probabilities for initiation, early-stage crack growth and dormancy[13)]. However, the failure cases of pipeline documented to date have been almost all old pipelines constructed in the early line pipe history, when pipeline steel was low grade and the coatings available were not of good quality. Moreover, the studies concerning crack initiation and early-stage growth are mainly from these low-grade steels. With the development of pipeline technology over the past several decades, pipeline steels are of much higher strength with thicker gauges to transport gas and oil under higher pressures due to the significant cost consideration. Thus, it is necessary to investigate crack initiation and early-stage propagation of these high grade steels to provide some useful reference to pipeline operation and management, and to reduce the likely incidents caused by SCC. At the same time, it is also of essence to determine which of the crack-initiation events stated above can give rise to the development of viable cracks and threaten the integrity of the pipeline; it is also essential to study the dynamics governing crack initiation, early-stage crack growth, dormancy, reactivation and coalescence.

Table 1. Chemical composition of X-80 pipeline steel (wt%).

C	Si	Mn	Cr	Ni	Mo	Cu	Al	Nb	V	Ti	P	S	Co	Ca
0.04	0.34	1.60	0.024	0.30	0.29	0.25	0.024	0.074	0.0048	0.012	0.011	0.002	0.008	<.001

Table 2. Mechanical properties of the X-80 pipeline steel .

Orientation	Yield Stress (0.2%), MPa	Ultimate Tensile Strength (MPa)	Elongation(%)	Reduction of area (%)
Transverse	661.6	697.5	25.7	76.2
Longitudinal	608.5	701.3	26.2	76.6

Experimental Procedures

Grade 522 (X-80) steel was used in this study. The chemical composition is shown in table 1. Tension teste on X-80 pipeline steel in both transverse and longitudinal direction were conducted in accordance with ASTM standard E8-01[14], and the mechanical properties for the two orientations are given in Table 2. The tensile specimens were machined from the unflattened segment of pipe. The mechanical properties in the transverse and longitudinal directions were almost the same, but the 0.2% yield stress demonstrated that the value in the transverse direction was 8.73% higher than that of the longitudinal direction.

Flat-coupon four-point bending specimens with dimensions of 60×20× 4 mm were machined from the unflattened segment of the pipe, and the length of the specimens was along the transverse direction of the pipe, the aim of which was to orient crack development in the test specimens in the same direction of the pipe as those observed in the field. All of the specimens were polished to 1 μm diamond finish, using non-aqueous coolant and oil-based diamond suspension, in order to avoid dissolving non-metallic inclusions during polishing. Cyclic loading tests were performed on four-point bending specimens by servo-pneumatic, as shown in Figure 1, in NS4 solution and actual soil solution purged with a 5% CO_2/N_2 mixture gas, respectively. The NS4 solution, containing (122 mg/L KC1, 483 mg/L $NaHCO_3$, 181 mg/L $CaCl_2 \cdot 2H_2O$, and 131, mg/L $MgSO_4 \cdot 7H_2O$, has been used widely to investigate transgranular SCC of pipelines. The balanced triangular waveform was employed in the tests, in the which the stress ratio (the ratio of minimum stress to maximum stress) was 0.82, the frequency was 0.0017 Hz and the maximum stress was 95% yield strength (YS). At the same time , the strain rate was kept at 2 × 10^{-6}/s so that the deformation rate in the tests was as close to that in the field as possible. All of the tests were at open circuit potential. Cyclic loading was applied to the specimens once the solution was bubbled with the mixture gas for about 4 h. The tests were interrupted after the desired numbers of load cycles for microscopic examination. All the specimens were cleaned using the rust remover containing 474.6 mL/L, HC1, 2 g/L hexamethylenetetramine ($C_6H_{12}N_{14}$) and 645.5 ml/L distilled water, before examination using scanning electron microscope (SEM). In addition, the energy-dispersive X-ray (EDX) was also used to analyze inclusions and other features.

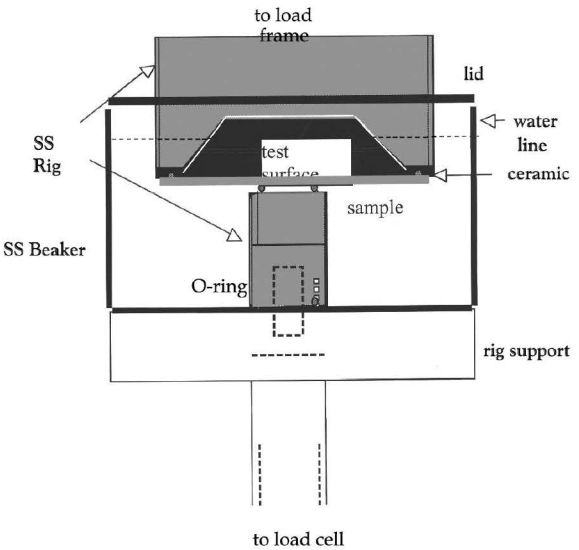

Fig. 1. 4-point bending test set-up.

Results and Discussion

SCC in Soil Solution Purged with 5% CO_2/N_2:

When X-80 pipeline steel specimens were loaded at a strain rate of 2E-6/s with a stress ratio of 0.82, frequency of 0.00173 Hz, and σ_{max}=0.95 yield strength in near-neutral-pH soil solution, it was found that there were only general corrosion features on the well-polished specimen surface after 2091 cycles, as shown in Figure 2. Some corrosion products were adhered to the specimen surface; however, at this time, it was likely that pitting would tend to form – that is to say, pitting incubation could occur. After 6128 cycles, many clusters of pits appeared on the surface of the specimen exposed to soil solution, some of which were about 100 μm in the pit-mouth

diameter and some of which were not deep enough (see Figure 3). Some iron carbonate deposits and other elements, such as Mn and Si, were also observed around the pits. This was revealed by EDX microanalysis, and the latter was related to non-metallic inclusion. In addition, the composition varied with the inclusions and the morphology of the pits was associated with the inclusion chemistry.

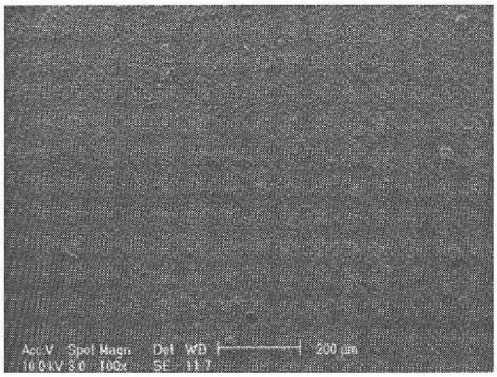

Fig. 2. Surface morphology of an X-80 pipeline steel specimen after 2091 cycles at σ_{max} =95% YS, R=0.82, F= 0.0017 Hz and a strain rate of 2×10^{-6}/s in soil solution purged with 5% CO_2/N_2,showing general corrosion.

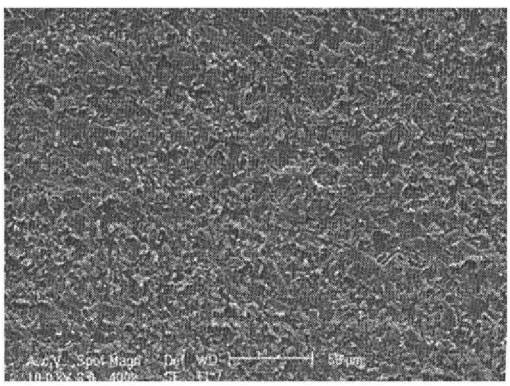

Fig. 3. Morphology of pits in an X-80 pipeline steel specimen after 6128 cycles at σ_{max} = 95%YS, R=0.82, F= 0.0017 Hz and a strain rate of 2×10^{-6}/s in soil solution purged with 5% CO_2/N_2,showing clusters of pits that had developed.

Whether an inclusion acted as an anode, or as an efficient cathode, causing the dissolution to be localized at the immediately adjacent matrix, pit development in the current system was a galvanic effect attributed to the different dissolution rates in different crystallographic directions[10]. The dissolution rate and the preferential corrosion direction depended on the nature of the solution to which the steel was exposed (i.e., in one particular crystallographic direction, the dissolution might be faster than in other directions in one solution, but slower in another solution)[10]. In polycrystalline metals, the orientation of a grain could influence the depth of the corrosion penetration, so that microscopic surface geometric discontinuities would be introduced; local corrosion cells could lead to surface geometric discontinuities. Because the physical – electrochemical behavior differed between the non – metallic inclusion and the matrix, the local corrosion cell was formed, and the different dissolution rates resulted in the formation of pits.

After 14373 cycles, more and more pits were observed on the specimen surface, as shown in Figure 4(a); some of these pits were very large and deep, (about 400. μm in mouth diameter)[see Figure 4(a)]. It was clearly seen that the original pits could grow in both depth and width. Some new pits might initiate and develop into large pits within the test time. At some locations, there were many more pits while at others, a limited number of pits, or even no pits, were observed. Some pits seemed to link together (see Figure 4(a) around the pits, inclusion was found; EDX analysis revealed that this inclusion was mainly composed of Mn and iron oxide, as shown in Figure 4(b), which implied that this kind of inclusion acted as a cathodic phase in galvanic corrosion. However, there was no crack or crack – like feature on the specimen surface at this time.

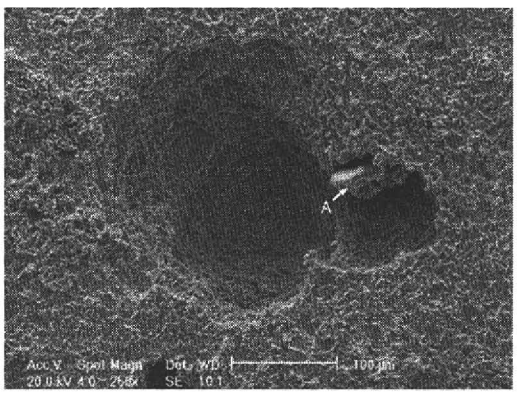

(a)

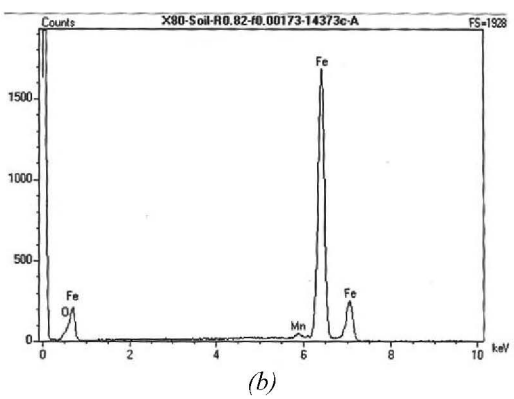

(b)

Fig. 4. The specimen surface morphology of an X-80 pipeline steel specimen in soil solution purged with 5% CO_2/N_2 at OCP with an R of 0.28 and a frequency of 0.00173 Hz for 14,373 cycles in a four-point bending test.

After 27,749 cycles, many cracks associated with pits were observed on the specimen surface, as shown in Figure 5. Some cracks initiated around the mouths of pits (see Figure 5) that were perpendicular to the stress axis, while some cracks were observed at the bottoms of pits (see Figure 6). At macro– scale, some pits 200 μm in diameter did not show any crack, however small cracks were observed at the bottom [see Figure 6(b)]. At this time, the transition from a pit to a crack or a crack embryo occurred.

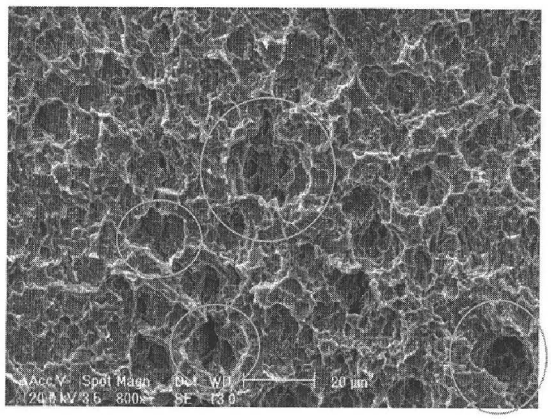

Figure 5. The morphology of cracks in an X-80 line pipe steel specimen after 27,749 cycles σ_{max} *= 95%YS, R=0.82, F=0.0017 Hz and a strain rate of 2×1010*$^{-6}$*/s in soil solution purged with 5%* CO_2/N_2*,showing cracks initiated around pits.*

It was clear that some pits about 20 μm in diameter could transform into cracks, as shown in Figure 5. However, there were no cracks around or at the bottom of some large pits, such as shown as location "A" in Figure 6(a). Kondo[15] first proposed the criterion about the transition from a pit to a crack; the cyclic stress intensity range for an equivalent (semi-circular) crack must exceed the fatigue crack growth threshold. Thus, the critical size of a pit to initiate a crack can be calculated as:

$$a_c = \frac{Q}{\pi\alpha}\left[\frac{(\Delta K)_p}{2.24\sigma_a}\right]^2 \qquad (1)$$

Where $(\Delta K)_p$ was the critical pit condition, σ_a was the stress amplitude, α was the aspect ratio a/b, Q was the shape factor $(1+1.464a^{1.65})$. No short crack correction factor was used in defining the critical pit size. This approach was subsequently adopted by Chen[16] with the only distinction being a slightly more elaborate relationship for the stress–intensity factor. If this criterion was used to investigate the transition in the current study, the critical size of a pit could be calculated. If $(\Delta K)_p$ = 1.0 MPa.m$^{1/2}$, the critical diameter of a pit was 101.6 mm. However, some cracks can initiate from the pits with about 20 μm. If $(\Delta K)_p$=0.5 MPa.m$^{1/2}$, the critical diameter of a pit was 25μm. Moreover, there were no cracks around some large pits (about 150 mm). So this criterion could not explain the phenomenon very well. Nevertheless, studies of the transition from pitting to corrosion fatigue growth (or crack nuclear) in aluminium alloys suggested that the pit size at transition was in the range of 40-200 μm[17]. For the specimen with pits, stress concentration around pits did exist, and sometimes the stress would be very high around these defects. According to the handbook[18], the stress concentration could be given by:

$$K_1 = C_1 + C_2(\frac{b}{t}) + C_3(\frac{b}{t})^2 + C_4(\frac{b}{t})^3 \qquad (2)$$

Where b was the pit depth, t was the specimen thickness, and

$$\left.\begin{aligned} C_1 &= 1.795+1.484(\tfrac{b}{a})-0.211(\tfrac{b}{a})^2 \\ C_2 &= -3.544-3.677(\tfrac{b}{a})+0.578(\tfrac{b}{a})^2 \\ C_3 &= 5.459+3.691(\tfrac{b}{a})-0.565(\tfrac{b}{a})^2 \\ C_4 &= -2.678-1.531(\tfrac{b}{a})+0.205(\tfrac{b}{a})^2 \end{aligned}\right\} \quad 0.5 \le \frac{b}{a} \le 2.0 \qquad (3)$$

$$\left.\begin{aligned} C_1 &= 2.966+0.502(\tfrac{b}{a})-0.009(\tfrac{b}{a})^2 \\ C_2 &= -6.475-1.126(\tfrac{b}{a})+0.019(\tfrac{b}{a})^2 \\ C_3 &= 8.023+1.253(\tfrac{b}{a})-0.020(\tfrac{b}{a})^2 \\ C_4 &= -3.572-0.634(\tfrac{b}{a})+0.010(\tfrac{b}{a})^2 \end{aligned}\right\} \quad 2.0 \le \frac{b}{a} \le 20.0 \qquad (4)$$

The calculated values are shown in Figure 7. if a/b=5, the stress was almost constant when the pit depth was less than 100 μm; after that, the stress would increase wit the pit depth. The stress around the pitting, 1308~1338 MPa; was very high relative to the yield stress. For a pit depth of 50 μm, stress decreased with the pit shape parameters, a/b [see Figure 7 (b)]. The stress varied from 2100~1250 MPa; at these levels, plastic deformation occurred around the pit, even plastic accumulation around these locations. In a benign condition, the transition from a pit to a crack would take place due to the accelerated dissolution caused by localized micro-plasticity.

As a matter of fact, the crack-initiation process was a competition between pitting and crack growth (assuming the crack-initiation process to be a dynamic process between pit development and crack growth), and it was characterized by the transition to crack growth from a growing corrosion pit[19]. When the time-based crack-growth rate exceeded the pit-growth rate, the crack could survive. Crack growth had to be feasible (the threshold must be exceeded) and must be greater than the pit growth rate. The growth rate of short cracks was not necessarily the

same as that of a long crack of the same stress intensity factor due to interactions with the microstructure, plastic wake effects in long cracks, and differences in chemistry and electrochemistry[20]. Crack growth might also occur below the threshold value determined from studies on long crack growth.

Under high stress ratio, low frequency, and low strain rate, (e.g 0.82, 0.0017, 2E-6s, respectively), conditions, which are very close to those of operational pipelines, SCC did occur in near-neutral-pH soil solution. Stress-corrosion crack initiation was associated with the solution constituents and physical-chemical properties.

Four-point Bending Tests in NS4 Solution Purged with 5% CO_2/N_2:

On the smooth specimen surface in NS4 solution purged with 5% CO_2/N_2, general corrosion only existed after 2091 cycles. After 6218 cycles, there were still general corrosion features on most of the specimen surface. At some locations, some pits were also observed. Compared to the results in Figure 3 for the case in soil solution, the pits in NS4 solution were much shallower and smaller, and limited in number. After 31062 cycles, the pits that formed previously disappeared, and there were no cracks on the specimen surface. Thus it seemed that soil solution was much more susceptible to pitting and SCC than NS4 solution. Beavers[21] also found the NS4 electrolyte was not as potent a cracking environment as actual field environments. Although the NS4 solution, or something similar, used by most researchers to simulate the environment that causes near-neutral-pH SCC in the field, many researchers have experienced difficulties in initiating SCC in that environment under realistic loading conditions and in obtaining reproducible results in terms of crack-growth rates. There have been several reports of unexpected and unexplained very high or very low-growth rates[22]. It is thus possible that there are some undiscovered constituents in the actual soil environment that may be critical in terms of SCC initiation and growth.

Before the tests started one specimen, was scratched. After 2091 cycles, the morphology from the replica showed clearly that the scratch was on the surface. However, the scratch disappeared with an increase in immersion time, reflecting that the surface discontinuity could be dissolved and SCC was related to the corrosion behavior of the steel in the environment.

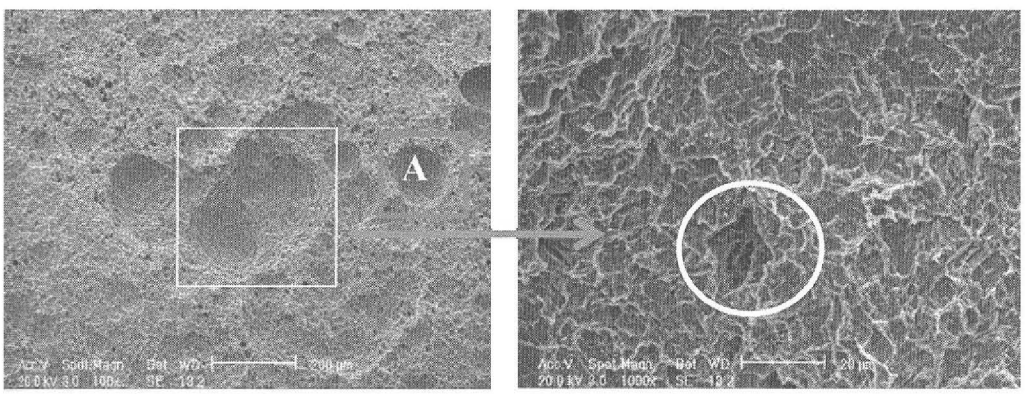

(a) (b)

Fig. 6. The morphology of cracks at the bottom of a pit in an X-80 line pipe steel specimen after 27,749 cycles σ_{max} = 95%YS, R=0.82, F=0.0017 Hz and a strain rate of 2×10^{-6}/s in soil solution purged with 5% CO_2/N_2.

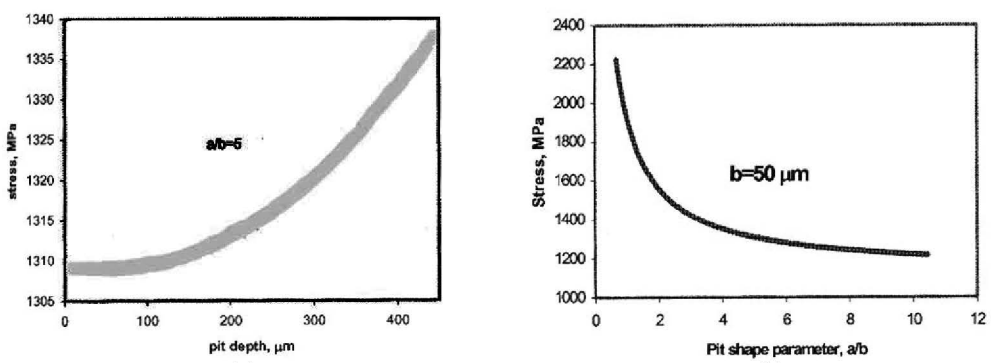

(a) (b)

Fig. 7. Stress distribution around a pit with (a) pit depth and (b) pit shape parameter.

Surface geometric discontinuities could cause stress concentration, and thus , micro-plastic deformation can occur around those discontinuities if an appropriate combination of the geometry of the discontinuity and stress conditions were achieved. Plastic deformation might enhance the dissolution rate, but since there was no passivation in the NS4 solution purged with 5% CO_2/N_2, dissolution was not restricted to localized plastically deformed regions. Dissolution could also facilitate plasticity. Cracking depended on the competition and interaction between dissolution and plasticity. If the stressing condition was too moderate, the critical amount of plastic deformation for crack initiation could not be achieved. If the enhanced dissolution rates at some local regions were not greater than the general corrosion rate, the crack could not form. If the solution were not corrosive, the stress concentration due to the dissolution of some non-metallic inclusions, and the plasticity effect, could not be reached, thus crack formation is prevented. However, if the solution corrosivity were severe, the environment would dissolve the sharp edges of some features associated with the geometric discontinuities. Thus, it might reduce the surface roughness and eliminate the regions that could cause stress concentrations. In order to initiate or grow a crack, crack activity should be maintained, or crack shape should be retained. The propagation rate at the crack tip, in both the surface and in the depth directions, must be greater than the rate of lateral dissolution along the crack walls, whether the driving force for the propagatio was chemical/ electrochemical, or mechanical.

Conclusion

Stress-corrosion cracking does occur in the laboratory in actual soil solution at high-stress ratio and low frequency, conditions close to those in the field. There are many pits and cracks on the specimen surface loaded in the soil solution, but only a limited number of small and shallow pits, and no cracks are observed in the NS4 solution. This indicates that the actual soil solution is more conclusive to pitting and SCC than the NS4 solution; this may be related to some undiscovered constituents in soil solution. When the pit reaches a critical size, the increased stress concentration around it will be very high; the local plastic accumulation occurs facilitating dissolution at the pit bottom or the mouth of the pit perpendicular to stress axis direction. At the benign combination between the mechanical and solution corrosivity, a pit will transform into a crack.

Acknowledgments

The authors acknowledge Clinton DeRushie, Yves Lafreniere, Michale Attard and Claude Marchand for their help.

Reference

[1] P. N. Parkins, Corrosion/2000, Paper No. 00363, NACE Int., 2000.
[2] T. N. Baker, C. G. Rochfort, R.N. Parkins, Oil and Gas J., 85 (1987), 37.
[3] B. Delanty, J. O'Beirne, Oil and Gas J. 90 (1992), 39.
[4] National Energy Board, Report of Public Inquiry Concerning Stress-Corrosion Cracking on Canadian Oil and Gas Pipelines, MH-2-95, 1996.
[5] R. N. Parkins, J. A. Beavers, Corrosion. Vol. 59, No. 3, Mar. 2003, 258-273.
6. X. Y. Zhang, S. B. Lambert, R. Sutherby and Plumtree, " Transgranular Stress-Corrosion Cracking of X-60 Pipeline Steel in Simulated Ground Water", Corrosion 59 (2003), 258.
[7] R. N. Parkins, W. K. J. Blanchard and B. S. Delanty, Corrosion, 50 (1994), 394.
[8] R. R. Fessler, K. Krist, Corrosion/2000, paper No. 00370, NACE Int., (2000).
[9] M. Elboujdaini, Y. Z. Wang, R. W. Reivie, R. N. Parkins and M. T. Shehata, Corrosion/2000, Paper No. 00379, NACE Int., (2000).
[10] Y. Z. Wang, R. W. Revie, M. T. Shehata, R.N. Parkins and K. Krist, Int. Pipeline Conf., ASME, (1998), 529.
[11] Y. Z. Wang, R. W. Revie, M. T. Shehata, R. N. Parkins, Materials for Resource Recovery and Transport, L. Collins, Editor, CIM, (1998), 71.
[12] M. Elboujdaini, Y. Z. Wang and R. W. Revie, 2000 Int. Pipeline Conf., ASME, (2000), 967.
[13] F. King, T. Jack, W. Chen, S. Wang, M. Elboujdaini, R. W. Revie, R. Worthingham and P. Desuk, Corrosion/2001, Paper No. 01214, NACE Int. (2001).
[14] ASTM Standard E8-01 "Standard Test Methods for Tension Testing of Metallic Materials", (2001).
[15] Y. Kondo, Corrosion, 45 (1989), 7.
[16] G. C Chen, C. M. Liao, K. C. Wan, M. Gao and R. P. Wei, ASTM STP 1298, (1997), 18.
[17] R. P. Wei, ASTM STP 1401, (2000), 3.
[18] W. D. Pikey, "Peterson's Stress Concentration Factors", 2nd Edition, NY, NY: Rexdale, Ontario, Wiley, (1997).
[19] R. P. Wei, D. G. Harlow, Proc. of Corros./2003 Research Topical Symp. Modeling and Prediction of Lifetimes for Corrodible Structures, 206.
[20] R. P. Gangloff, R. O. Ritchie, Fundamentals of Deformation and Fracture, K. J. Miller, Editor, Cambridge University Press, (1984).
[21] J. A. Beavers, C. L. Durr, B. S. Delanty, D. M. Owen and R. L. Sutherby, Corrosion/2001, Paper No.01217 NACE Int., (2001).
[22] Michael Baker Jr., Ink., Integrity Management Program ,(2004).